

Two-photon excitation in living cells induced by low-power CW laser beams

Karsten König^{1,2}, Tatjana Krasieva³, Yagang Liu³, Michael W. Berns³, Bruce J. Tromberg³

¹Institute of Anatomy II, Friedrich Schiller University, D-07743 Jena, Germany

²Institute of Molecular Biotechnology, D-07708 Jena, Germany

³Beckman Laser Institute and Medical Clinic, University of California, Irvine, CA 92715

1. ABSTRACT

We demonstrate multi-photon excitation in optically-trapped living cells. Intracellular non-resonant two-photon excitation of endogenous and exogenous chromophores was induced by CW near infrared (NIR) trapping beams of 105 mW power. In the case of fluorescent chromophores, detection of NIR-excited visible fluorescence was achieved by imaging and spectroscopy methods. Trap-induced, two-photon excited fluorescence was employed as a novel diagnostic method to monitor intracellular redox state and cell vitality of single motile spermatozoa and Chinese hamster ovary cells. We found, that nonlinear absorption of NIR photons <800 nm may lead to oxidative stress and severe cell damage. Biological response was amplified in multimode CW lasers due to longitudinal mode-beating and partial mode-locking. As a result, we recommend the use of longwavelength-NIR, single-frequency traps ("optical tweezers") for micromanipulation of vital cells.

Keywords: optical trapping, NIR, microbeam, NADH, oxidative stress, photodamage
two-photon excited fluorescence, multi-photon excitation

2. INTRODUCTION

Optical trapping, based on force generation during laser beam refraction in micrometer-sized samples, is a novel method in vital cell micromanipulation^{1,2}. A highly focused CW laser beam (microbeam) serves as the trapping beam. In order to avoid intracellular heating by absorption, trapping wavelengths are in the near infrared (NIR, 700 - 1200 nm). A large number of trapping studies have been conducted using CW Nd:YAG lasers at 1.06 μm . Tunable Ti:Sapphire and diode lasers are used for optical trapping at shorter NIR wavelengths where water absorption is reduced³. This effect could be particularly beneficial in the case of motile cell trapping where trapping forces have to be higher than the ATP-driven intrinsic motility forces. Laser powers of 50-150 mW are typically required for confinement of highly motile spermatozoa⁴.

Optical trapping has been proclaimed to be a non-invasive method. For example, the use of optical traps for laser-assisted in vitro fertilization in the case of male infertility has been suggested⁵⁻⁷.

In 1994, we found that optical traps are sources of multiphoton excitation^{8,9}. When 50-150 mW CW laser beams are focused to diffraction-limited spots, trapping intensities of 15-40 MW/cm² (750-1064 nm) and photon flux densities of $\approx 10^{27}$ cm⁻²s⁻¹ are generated. With typical 10⁻⁵⁰ cm⁴s molecular two-photon absorption cross sections^{10,11}, two-photon excitation processes are efficiently induced¹².

Two-photon excited fluorescence induced by CW beams has been reported¹³. However, there was no report on nonlinear chromophore excitation by optical traps and its biological consequence for vital cell micromanipulation. In this paper we summarize our studies on trap-induced two-photon excitation of intracellular endogenous and exogenous chromophores.

3. MATERIALS AND METHODS

Cells

Chinese hamster ovary cells (CHO, ATCC no. 61) were maintained in GIBCO's minimum essential medium (MEM, 10% fetal bovine serum). For trapping, trypsinized cells were injected into modified Rose cell culture chambers. Semen specimens were obtained from three donors with normal semen parameters according to the World Health Organization guidelines. Semen was diluted in HEPES buffered isotonic saline solution containing 1% human serum albumin and injected into similar microchambers.

In vitality experiments, cells were stained with a Live/Dead kit containing the live-cell stain SYBRTM14 with a 515 nm fluorescence maximum and the dead-cell stain Propidium Iodide (PI) emitting in the red.

Experimental setup for CW studies

The NIR radiation of an Ar⁺-ion laser-pumped tunable CW Ti:Sapphire ring laser (Coherent, 899-01) was introduced into a modified inverted confocal laser scanning microscope (CLSM, Axiovert 135M, Zeiss). The parallel beam was expanded to fill the back aperture of a 100x Zeiss Neofluar brightfield objective (NA=1.3). The microscope allowed trapping of single cells and simultaneous fluorescence imaging; either by scanning with 488 nm argon ion laser microbeams, by detection with a slow-scan, cooled CCD camera (TE576/SET135, Princeton Instruments), or by sensitive color video imaging (ZVS-47DEC, Zeiss).

The power measured in air near the focal plane was multiplied by a 1.5 correction factor, which accounts for different refractive indices (immersion, glass, medium), to obtain *in situ* powers (power at the sample)¹⁴. A mean trapping efficiency parameter $Q = 0.12$ at 800 nm for human spermatozoa and this particular experimental setup was determined recently using an appropriate hydrodynamic model for ellipsoidal specimens¹⁴.

Fluorescence spectra were obtained with another experimental setup, which consists of a 1064 nm trapping beam and a polychromator combined with a cooled optical multichannel analyzer for spectra recording. Each spectrum was acquired in 5 s. The setup is described in detail in refs.(15, 16).

4. RESULTS

4.1. Two-photon excited fluorescence

Highly focused CW 105 mW NIR beams at 750 nm, 760 nm, 780 nm, 800 nm, and 1064 nm were employed to trap single motile sperm cells as well as immotile CHO cells. Cells were labeled with the live-cell fluorophore SYBRTM14. At all trapping wavelengths, cells exhibited an intracellular green spot which was visible by observation through eyepieces, indicating trap-induced two-photon excited fluorescence. The spot also marked the trapping beam position, which in the case of trapped sperm was found to be in the lower part of the sperm head. Fluorescence imaging revealed spot position variations and a $<0.5 \mu\text{m}$ spot size, Fig. 1. The spot position was not constant over time due to time-dependent sperm activity (transient hyperactivity, mean motility reduced with trapping time). In some cases, transient trapping beam location near the sperm midpiece was detected. Additional incubation with the fluorophore PI resulted in spot color change from green into red after certain trapping times for $<800 \text{ nm}$ traps (see section 4.2.).

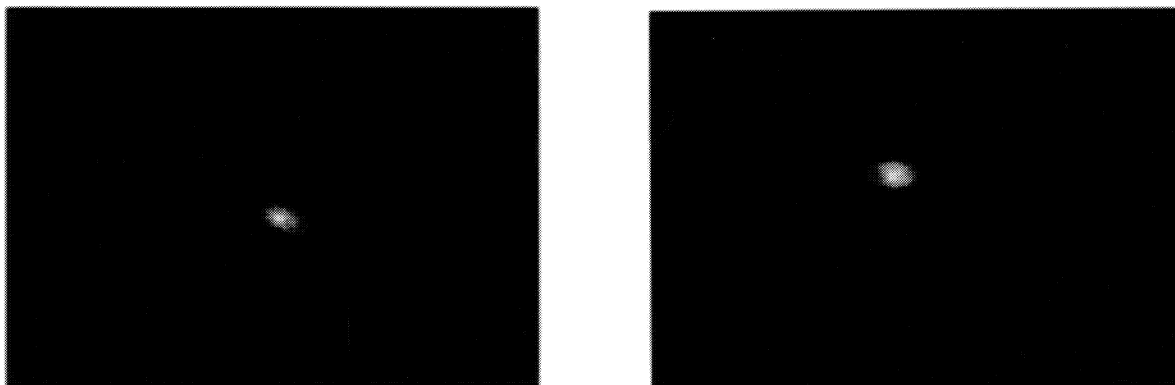


Fig. 1 Trap-induced two-photon excited fluorescence spot with submicron dimensions in sperm head. In order to visualize the sperm position with respect to cell boundaries, additional bright-field illumination with white light (halogen lamp) or, as shown, with fluorescence excitation light from the mercury lamp was applied. The intensity of trap-induced two-photon excited fluorescence of intracellular SYBR, PI, or Acridine Orange was high enough to be recognized in spite of additional one-photon excited fluorescence.

The flux of trap-induced fluorescence photons can be estimated as follows:

For photon flux densities of $\approx 10^{27} \text{ cm}^{-2}\text{s}^{-1}$, an assumed $10^{-50} \text{ cm}^4\text{s}$ molecular two-photon absorption coefficient, and a fluorescence quantum yield ~ 1 of an exogenous fluorophore, fluorescence signals of $10^2 - 10^4$ photons/s per molecule can be generated in $\approx 300 \text{ nm} \times 300 \text{ nm} \times 900 \text{ nm}$ trapping spots ($\approx 0.1 \text{ }\mu\text{m}$ volume). For 10^{-5} M dyes (≈ 600 molecules per spot) and instrument efficiencies on the order of 1%, this corresponds to detector count rates of 10^3 to 10^5 s^{-1} . These signal levels can be measured using a variety of commercially-available detector systems and are generally in the range of ocular sensitivity. In the case of endogenous fluorophores, such as NAD(P)H, the fluorescence quantum yield can be assumed to be ≈ 0.01 , and therefore, fluorescence photon flux will be 2 orders of magnitude lower. However, exact molecular two-photon absorption cross sections and two-photon fluorescence quantum yields of most of fluorophores are not known.

4.2. Trap-induced cell damage

Sperm confined in the trap tried to escape as seen by flagellar motions. In general if successful, sperm escaped in general in the direction of movement prior to trapping ("memory effect"). In <10% of trapped sperm, cells lost their initial orientation and started to rotate around optical axis.

In the case of <800 nm traps (105 mW), sperm trapping resulted in a rapid decrease of ATP-driven motility. This decrease was superposed in some individual sperm cell by transient hyperactivity and short-term rests. Finally, flagellar motion of the trapped cell stopped completely (paralysis).

In order to estimate the trap-induced mean decrease of intrinsic motility force, the laser power was step-wise reduced until the cell was able to escape. This so-called minimum trapping power P_{\min} was used to calculate the corresponding trapping force F_{trap} and the motility force F_m , respectively, according:

$$F_{\text{trap}} = F_m = Q P_{\min}/c,$$

where a constant Q value in the wavelength range 750-800 nm of 0.12 was assumed, and $c = 2.25 \times 10^8 \text{ ms}^{-1}$ is the light speed in medium. A mean motility force of 44 pN was determined for spermatozoa prior to long-term trapping stress. Results are listed in the Table.

In order to determine if trapping may result in cell killing, the well-known indicator Trypan Blue (TB) was added to the medium. Observation of trap-induced intracellular TB accumulation was performed by brightfield imaging, using the white radiation of the halogen microscopy lamp. We detected cell killing in 760 nm traps with 2 minutes of trapping (105 mW).

A more sensitive method is the use of a fluorescent dead-cell stain such as PI. Excitation of PI and SYBR fluorescence is possible with radiation at several lines of the high-pressure mercury lamp. In combination with sensitive color video imaging we were able to video-tape intracellular accumulation sites of SYBR and PI in trapped sperm and to monitor spatially-resolved kinetics of trap-induced color changes. We found that onset of PI occurred in the lower head part and that PI fluorescence spread within some seconds into the entire head. In order to create higher resolution and higher contrast PI fluorescence images, confocal laser scanning fluorescence microscopy in combination with trapping was employed (Fig. 2). Because the scanning beam, as well as the trapping beam are transmitted through the same objective, 3D imaging is impossible with this one-objective setup. Nevertheless, confocal images can be obtained in one z-plane. The position of this plane within the sample is defined by the focal plane of the 488 nm excitation beam and the focal plane differences between 488 nm and NIR trapping radiation. This chromatic aberration depends on the objective. However, focal plane matching is possible by changing the entrance angle of a beam entering the objective. Unfortunately, this results in loss of ability to focus to diffraction-limited spots.

In our opinion, the most elegant method to probe cell vitality is imaging of two-photon excited PI fluorescence. As mentioned, the position of the trapping beam is inside the sperm head (near the cell center in CHO cells), where nucleic acids are present and therefore, PI accumulation occurs. Due to the rapid dye diffusion within the head, onset of PI fluorescence at different intrahead positions is nearly the same. The main advantage of this novel diagnostic method is the fact, that no external light sources are needed and photochemical effects, such as by photodynamic activity of PI, can be excluded. The NIR beam is not able to induce photodynamic PI activity in living cells, because vital cells are able to exclude PI and the trapping position (and consequently two-photon excitation) is inside the cell.

We found that trap-induced cell death occurred in <800 nm traps within 10 min. The strongest effect was found for 760 nm traps (≈ 1 min). The onset of two-photon excited PI fluorescence during sperm trapping is listed in the Table.

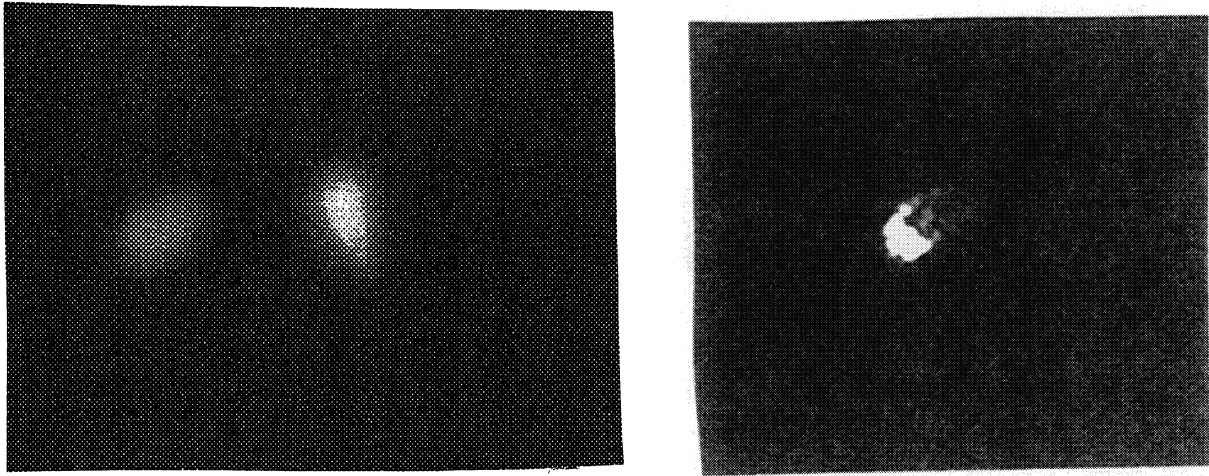


Fig. 2 Confocal laser scan images of SYBRTM14 and PI labeled 760nm-trapped sperm cells.
 a) detection: 510-525 nm, 10 s trapping b) detection: 630-700 nm, 1 min trapping

λ /nm	F_m (2min) /pN	tPI /s
750	5	170
760	0	60
770	8	180
780	21	550
800	33	>600

Table. Mean motility forces F_m after 2 min trapping and onset of intracellular PI accumulation (tPI).

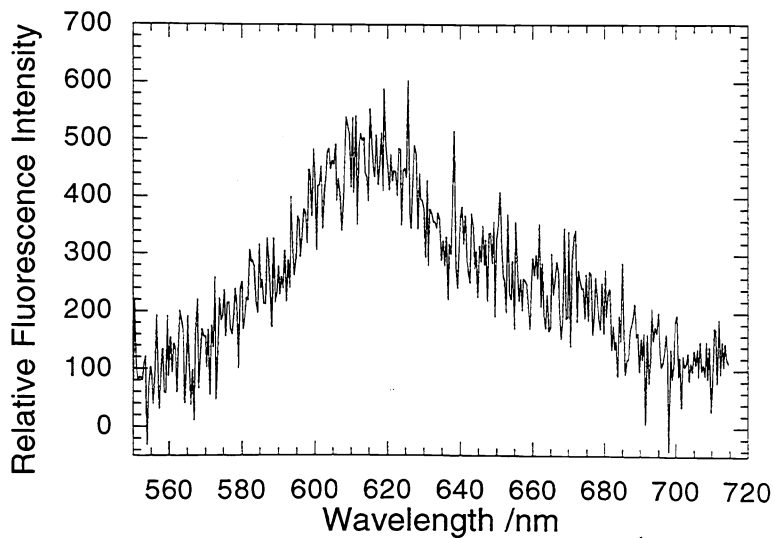


Fig. 3 Two-photon excited intracellular PI spectrum ($\lambda_{exc}=1064$ nm)

A final indicator of trap-induced cell damage was given by autofluorescence measurements in the blue spectral range. Intracellular autofluorescence originates from endogenous fluorophores, such as the fluorescent reduced coenzymes β -nicotinamide adenine dinucleotide (NADH) and β -nicotinamide adenine dinucleotide phosphate (NADPH), denoted here as NAD(P)H. Free NAD(P)H absorbs around 340 nm and fluoresces around 460 nm, whereas bound NAD(P)H exhibits a blue-shifted fluorescence maximum around 440 nm. The oxidized form NAD(P) exhibits no fluorescence. The NAD(P)H fluorescence acts as indicator for cellular metabolism and reflects the intracellular redox state^{17,18}. We monitored modifications of cellular autofluorescence to obtain information on trap-induced cell damage. Confined in an 800 nm trap, unlabeled sperm cells exposed to 5 s UVA light (365 nm) of the mercury lamp exhibited weak autofluorescence. Autofluorescence was mainly localized in the cell mid-piece, the primary site of mitochondria. As "cellular power plants", mitochondria contain the highest NADH concentration inside a cell. In order to obtain good-quality images of the cell including flagellum from one object plane, the stage was slowly moved to force the cell to align along stream lines. A second image, taken after 10 min trapping at 800 nm, demonstrated no changes of autofluorescence pattern. In contrast, the second image after 760 nm trapping revealed a significant autofluorescence increase ($\approx 10x$) and relocalization of autofluorescence. The cell head became the brightest fluorescence site. In the case of 760nm-trapped CHO cells, strongest autofluorescence increase occurred near the trapping beam position and spread with time over the entire cell.

Two-photon excited autofluorescence confirmed these findings. We found an increase of the spot intensity up to two orders in 760 nm traps. At radiant exposures of about 10 GJ/cm^2 , the blue/green autofluorescent spot became clearly visible (eyepieces). No autofluorescence modifications were found in the case of 800 nm-trapped cells. 800 nm traps (105 mW) induced a weak autofluorescence signal. It should be noted, that two-photon excitation spectra of fluorophores may differ from one-photon excitation spectra (times two).

The 100fold increase of trap-induced sperm autofluorescence in contrast to 10fold UVA-induced mean cellular emission has its explanation in different excitation sites. As mentioned, the intrahead trapping beam is unable to excite NAD(P)H in healthy sperm efficiently (only during transient interaction with the sperm midpiece). Therefore, the trap-induced autofluorescence signal is low. However, if NAD(P)H accumulates in the sperm head, efficient fluorescence excitation is given.

The cell damage induced by NIR microbeams was compared with UVA-induced biological response. It is well-known that UVA exposure to living cells may induce radical formation and singlet oxygen generation, i.e. oxidative stress¹⁹. One potential photosensitizer for these photooxidation processes is NAD(P)H^{20,21}.

For comparable UVA studies (one-photon excitation), we used the 365 nm fluorescence excitation radiation of the mercury lamp. An UVA intensity of 3.5 W/cm^2 was determined (1 mW power, 0.19 mm spot). Confined in an 800 nm trap (no trap-induced damage), sperm cells were exposed to UVA up to 10 min. We found similar biological response as for 760 nm traps. At first, the motility force decreased. Paralysis occurred at a mean exposure time of 110 s, intracellular PI accumulation at 310 s. Paralysed unlabeled sperm showed exact same autofluorescence increase and head fluorescence.

In order to probe if the observed head fluorescence indicates NAD(P)H and not the formation of a new fluorophore, we measured the autofluorescence spectrum. We found the same spectral characteristics at the beginning and after 5 min UVA exposure, but with different intensities. Intracellular spectra with a band maximum at 440-460 nm are typical for NAD(P)H.

We conclude that NIR microbeams are able to induce oxidative stress via two-photon excitation of endogenous chromophores.

4.3. Amplification of biological response in multimode lasers

As seen from the Table, the most dramatic effect occurred in 760 nm traps. Interestingly, 750 nm traps induced lower biological response. We assumed that the observed dramatic effects in 760 nm traps depend somehow on the trapping laser.

In a first step to clarify the laser influence, we used a CW Nd:YAG laser at 1064 nm as alternative trapping source (105 mW). A mercury lamp (365 nm) served as fluorescence excitation source, fluorescence was detected as spectrum. We were able to confine sperm cells and CHO cells for 10 min without changes of intracellular redox state, onset of paralysis, or even PI accumulation. Therefore, 1064 nm traps (105 mW) worked as safe micromanipulation tools.

In order to probe if the 1064 nm trapping beam is capable to induce two-photon excited fluorescence, PI labeled spermatozoa were exposed to additional UVA light. Simultaneously, UVA-excited fluorescence spectra were measured. We found indeed UVA-induced onset of PI emission in the sperm head as well as in trapped CHO cells. In a next step we extinguished the mercury lamp. We were able to measure trap-induced, two-photon excited fluorescence spectra. A better signal-noise ratio was obtained by power increase (Fig. 3).

By monitoring the output of our CW Ti:Sapphire laser with an 1 GHz avalanche photodiode we found the presence of unstable ultrashort pulses in the sub-nanosecond region. Pulse repetition frequencies appeared at multiples of 180 MHz which corresponds to the cavity length of the ring laser. Interestingly, highest peak powers were obtained at the 760 nm birefringent filter position. With a linewidth of up to 20 GHz of the tunable element, 111 longitudinal cavity modes may contribute to pulse generation. Thus, under mode-locking conditions, longitudinal mode beating could produce 50 ps pulses.

Since two-photon excitation is proportional to squared peak power, biological effects are therefore most efficient at 760 nm. A final proof was given by introduction of an etalon into the Ti:Sapphire laser cavity which resulted in a single frequency trapping beam ("true CW trap"). Now, we were able to minimize the biological effect at 760 nm, however, we could not avoid cell death. Using 760 nm "true CW" traps, PI accumulation occurred at 406 s vs. 60 s in multimode CW traps at same 105 mW power.

5. DISCUSSION

Laser microbeams have been widely employed in biology and medicine as non-contact sterile tools for micromanipulating cells and monitoring cellular physiology. For example, high-peak-power, pulsed laser microbeams are used as microsurgical devices for cutting and inactivating cells and subcellular organelles ("optical scissors"). In contrast, CW microbeams are employed in laser scanning microscopes for imaging and in optical traps ("laser tweezers") for cell confinement and micromanipulation.

We proclaim that "laser scissors" as well as "laser tweezers" are sources of multi-photon absorption. In the case of shortwavelength-NIR microbeams, nonlinear excitation may result in oxidative stress and cell damage. Otherwise, multi-photon excitation of intracellular fluorophores can be used as a novel method in fluorescence diagnostics of single living cells.

6. REFERENCES

1. A. Ashkin, "Acceleration and Trapping of Particles by Radiation Pressure," *Phys. Rev. Lett.* 24(1970)156-159.
2. A. Ashkin, J.M. Dziedzic, J.E. Bjorkholm, and S. Chu, "Observation of a single-beam gradient force optical trap for dielectric particles," *Opt. Lett.* 11(1986)288-290.
3. G.M. Hale and M.R. Querry, "Optical Constants of Water in the 200-nm to 200- μ m wavelength region," *Appl. Opt.* 12(1973)555-563.
4. L.M. Westphal, I. El Dansasouri, S. Shimitzu, Y. Tadir, and M.W. Berns, "Exposure of human spermatozoa to the cumulus oophoruse results in increased relative force as measured by a 760 nm laser optical trap," *Human Reprod.* 8(1993)1083-1086.
5. Y. Tadir, W.H. Wright, O. Vafa, T. Ord, R.H. Asch, and M.W. Berns, "Micromanipulation of sperm by laser generated optical trap," *Fertil. Steril.* 52(1989)870-873.
6. J.M. Colon, P. Sarosi, P.G. McGovern, A. Ashkin, J.M. Dziedzic, J. Skurnick, G. Weiss, and E.M. Bonder, "Controlled micromanipulation of human sperm in three dimensions with an infrared laser optical trap: effect on sperm velocity," *Fertil. Steril.* 57(1992)695-698.
7. K. Schütze and A. Clement-Sengewald, "Catch and move - cut or fuse", *Nature.* 368(1994)667-669.
8. K. König, Hong L., Berns, M. W., and B.J. Tromberg, "Cell damage by near-IR microbeams." *Nature* 377(1995)20-21.
9. K. König, Y. Liu, T. Krasieva, P. Patrizio, Y. Tadir, G.J. Sonek, M.W. Berns, and B.J. Tromberg, "Invited Paper: Fluorescence imaging and spectroscopy of motile sperm cells and CHO cells in an optical trap ("laser tweezers")", *Proc. SPIE* 2391(1995)238-249.
10. J.P. Hermann and J. Ducuing, "Absolute Measurement of Two-Photon Cross Sections", *Phys. Rev. A* 5(1972)2557-2568.
11. S.M. Kennedy and F.E. Lytle, "p-Bis(o-methylstyryl)benzene as a power squared sensor for two-photon absorption measurements between 537 and 694 nm", *Anal. Chem.* 58(1986)2643-2647.
12. M. Göppert-Meyer, "Über Elementarakte in zwei Quantensprüngen," *Ann. Phys.* 9(1931)273.
13. P.E. Hänninen, E. Soini, and S.W. Hell, "Continuous wave excitation two-photon fluorescence microscopy", *J. Microsc.* 176(1994)222-225.
14. K. König, L. Svaasand, Y. Liu, G.J. Sonek, P. Patrizio, Y. Tadir, M.W. Berns, and B.J. Tromberg, "Determination of intrinsic forces of human spermatozoa using an 800 nm optical trap", submitted.
15. Y. Liu, D. Cheng, G.J. Sonek, B. J. Tromberg, and M.W. Berns, "A microspectroscopic technique for the determination of localized heating effects in organic particles", *Appl. Phys. Lett.* 65(1994)919.
16. K. König, Y. Liu, G.J. Sonek, M.W. Berns, and B.J. Tromberg, "Autofluorescence Spectroscopy of optically-trapped cells", *Photochem Photobiol.* 62(1995)830-835.
17. B. Chance and B. Thorell, "Localization and kinetics of reduced pyridine nucleotides in living cells by microfluorimetry.", *J. Biol. Chem.* 234(1959)3044-3050.
18. K. König and H. Schneckenburger, "Laser-Induced autofluorescence for medical diagnosis", *J. Fluorescence* 4(1)(1994)17-40.
19. R.M. Tyrell and S.M. Keyse, "The interaction of UVA radiation with cultured cells," *J. Photochem. Photobiol.* 4(1990)349-361.
20. M.L. Cunningham, J.S. Johnson, S.M. Giovanazzi, and M.J. Peak, "Photosensitized production of superoxide anion by monochromatic (290-405 nm) ultraviolet irradiation of NADH and NADPH coenzymes," *Photochem. Photobiol.* 42(2)(1985)125-128.
21. T.G. Burchuladze, E.G. Sideris, and G.I. Fraikin, "Sensitized NADH formation of single-stranded breaks in plasmid DNA upon the action of near UV radiation," *Biofizika.* 35(1990)722-725.